Journal of Solid State Chemistry **159,** 186–190 (2001)
doi:10.1006/jssc.2001.9149, available online at http://www.idealibrary.com on IDEAL®

$Gd_3Cu_2Te_7$ and $U_2Cu_{0.78}Te_6$: Two Examples of Linear Te Chains

Fu Qiang Huang and James A. Ibers[1]

Department of Chemistry, Northwestern University, 2145 Sheridan Road, Evanston, Illinois 60208-3113

Received December 4, 2000; accepted March 15, 2001; published online May 11, 2001

The compounds $Gd_3Cu_2Te_7$ and $U_2Cu_{0.78}Te_6$ have been synthesized by reactions of the elements at 1123 K in a KI flux. $Gd_3Cu_2Te_7$ crystallizes in the orthorhombic space group *Cmcm* with four formula units in a cell of dimensions $a = 11.4994(8)$, $b = 19.170(1)$, and $c = 6.1251(4)$ Å at $T = 153$ K. $Gd_3Cu_2Te_7$ can be considered to consist of one-dimensional isolated Te chains and two-dimensional ${}^2_\infty[Cu_2Te_5]$ layers separated by Gd atoms along the *b* axis. $U_2Cu_{0.78}Te_6$ crystallizes in the monoclinic space group $P2_1/m$ with one formula unit in a cell of dimensions $a = 6.100(1)$, $b = 4.2150(7)$, $c = 10.365(2)$ Å, and $\beta = 98.978(3)^\circ$ at $T = 153$ K. $U_2Cu_{0.78}Te_6$ contains two-dimensional ${}^2_\infty[UTe_3]$ layers joined by Cu atoms along the *c* axis. In both structures the Gd and U atoms are coordinated to bicapped trigonal prisms of eight Te atoms, and the Cu atoms are coordinated to tetrahedra of four Te atoms. Both structures contain linear Te chains. © 2001 Academic Press

INTRODUCTION

Lanthanide (*Ln*) or actinide (*An*) polychalcogenides LnQ_2, LnQ_{2-x}, Ln_2Q_5, LnQ_3, UTe_2, U_2Te_5, UQ_3, ThQ_3 (Q = Se, Te) have attracted attention because these materials are near the metal–insulator boundary and often exhibit interesting dimensionality, magnetism, and charge density wave behavior (1–6). Lanthanide polychalcogenides have layered structures with distorted rocksalt *LnQ* slabs separated by single or double planar square lattice sheets of the *Q* atoms (7–16). These *Q* atoms in the sheets are bonded to four neighboring *Q* atoms. Actinide polychalcogenides, except for β-UTe_3 ($NdTe_3$-type) (17), contain infinite distorted linear chains of *Q* atoms that alternate in their separations (18–20). Recently, some ternary and quaternary lanthanide and actinide polychalcogenides have been synthesized. Some contain distorted square *Q* nets, for example $Rb_{0.33}DySe_{2.66}$ (1), ALn_3Te_8 (A = K, Rb, Cs; Ln = Ce, Nd) (21), $KCeCuTe_4$ (22), $EuCu_{0.66}Te_2$ (23), $KEuCu_2Te_4$ (23), and $Na_{0.2}EuAg_{2.8}Te_4$ (23). Others contain infinite linear chains of *Q* atoms, for example $LnCu_xTe_2$ (Ln = La to Dy; x = 0.28 to 0.40) (24, 25), $Dy_3Cu_2Te_7$ (26), $Tl_{1.12}U_2Te_6$ (27), ATh_2Q_6 (A = K, Rb, Cs; Q = Se, Te) (28–30), Th_2CuTe_6 (31), $Rb_2CeCu_3Te_5$ (32), and $CsTiUTe_5$ (33). The chalcogen atoms appear to be equally spaced only in $LnCu_xTe_2$ (24, 25), $Dy_3Cu_2Te_7$ (26), and $CsTiUTe_5$ (33). We report here the syntheses and structures of the compounds $Gd_3Cu_2Te_7$ and $U_2Cu_{0.78}Te_6$; both structures contain linear undistorted Te chains.

EXPERIMENTAL

Syntheses

The following reagents were used as obtained: Gd (Alfa, 99.9%), U (Alfa, 99.7%), Cu (Alfa, 99.999%), and Te (Aldrich 99.8%). The compound $Gd_3Cu_2Te_7$ was prepared by the reaction of 1.0 mmol Gd, 0.67 mmol Cu, 3.0 mmol Te, and 400 mg KI flux. The compound $U_2Cu_{0.78}Te_6$ was prepared by the reaction of 0.50 mmol U, 0.25 mmol Cu, 1.5 mmol Te, and 200 mg KI flux. These mixtures were loaded into fused-silica tubes under an Ar atmosphere in a glove box. The tubes were sealed under a 10^{-4} Torr atmosphere and then placed in a computer-controlled furnace. They were kept at 1123 K for 72 h and then cooled at 0.3 K/h to 298 K. The reaction mixtures were washed free of iodide salt with water and then dried with acetone. In the first reaction, the major component consisted of black needles. In the second reaction, the major component was composed of golden–green needle-like plates. Analysis of these crystals with an EDX-equipped Hitachi S-4500 SEM showed the presence of only Gd, Cu, and Te in the ratio of approximately 3:2:7 for the black needles, and the presence of only U, Cu, and Te in the ratio of approximately 1:0.35:3 for the golden-green plates. These compounds are stable in air. $U_2Cu_{0.78}Te_6$ can also be synthesized with the use of excess elemental Te as a flux.

Structure Determinations

Single-crystal X-ray diffraction data were collected with the use of graphite-monochromatized Mo$K\alpha$ radiation

---

[1] To whom correspondence should be addressed.

0022-4596/01 $35.00

($\lambda = 0.71073$ Å) at 153 K on a Bruker Smart-1000 CCD diffractometer (34). The collection of the intensity data was carried out with the program SMART (34). Cell refinement and data reduction were carried out with the use of the program SAINT (34), and face-indexed absorption corrections were performed numerically with the use of the program XPREP (35). Then the program SADABS (34) was employed to make incident beam and decay corrections. The original data sets were collected with 15-s frame exposures. Since supercells might exist in these systems, 30-s frame exposures were employed in the collection of three groups of frames. No evidence for supercells was found.

The structures were solved with the direct methods program SHELXS and refined with the full-matrix least-squares program SHELXL of the SHELXTL-PC suite of programs (36). The refinement of the U structure was straightforward, with the final composition from the X-ray determination being $U_2Cu_{0.78(1)}Te_6$. For the Gd structure, refinement in space group *Cmcm* led to a structure with stoichiometry $Gd_3Cu_2Te_7$ that contained two nonequivalent Cu sites, with Cu1 fully occupied and Cu2 half occupied. The values of U_{33} for Cu1 and Cu2 are 0.068 and 0.121 Å^2, respectively. All other principal mean-square atomic displacements in the structure are normal. The $R1$ index is 0.0268. Refinement of the structure in space group $Cmc2_1$ led to a Flack parameter of 0.39(9), and U_{33} values of 0.070 and 0.174 Å^2 for atoms Cu1 and Cu2, respectively, and to a value of $R1$ of 0.0249. The positions of the other atoms shifted minimally from those in space group *Cmcm*. Thus, the large values of U_{33} persist and there is no convincing support for the choice of the lower symmetry space group. The Cu2 position is half occupied with the Cu2–Cu2′ distance being 1.601(9) Å, where atom Cu2 is at $x, y, \frac{1}{4}$ and atom Cu2′ is at $-x, y, \frac{1}{4}$. Clearly, these two positions cannot be occupied simultaneously in a given unit cell. The large values of U_{33} for the Cu atoms, especially for atom Cu2, are possibly a manifestation of the mobility of these Cu^+ ions in the [001] direction at the formation temperature of the structure, with a resultant distribution of positions as the

TABLE 1
Crystal Data and Structure Refinements for $Gd_3Cu_2Te_7$ and $U_2Cu_{0.78}Te_6$

Compound	$Gd_3Cu_2Te_7$	$U_2Cu_{0.78}Te_6$
formula weight	1500.45	1292.49
Space group	D_{2h}^{17}-*Cmcm*	$C_{2h}^{2} - P2_1/m$
a (Å)	11.4994(8)	6.100(1)
b (Å)	19.170(1)	4.2150(7)
c (Å)	6.1251(4)	10.365(2)
β (°)	90	98.978(3)
V (Å^3)	1350.2(2)	263.22(8)
Z	4	1
T(K)	153 (2)	153 (2)
λ(Mo$K\alpha_1$) (Å)	0.71073	0.71073
ρ_{calcd} (g/cm^3)	7.340	8.154
lin. abs coeff (cm^{-1})	324.04	485.15
$R(F)^a$ ($F_o^2 > 2\sigma(F_o^2)$)	0.0268	0.0235
R_w $(F_o^2)^b$ (all data)	0.0645	0.0576

[a] $R(F) = \sum||F_o| - |F_c||/\sum|F_o|$, and $F_o^2 > 2\sigma(F_o^2)$.

[b] $R_w\ (F_o^2) = [\sum\ w(F_o^2 - F_c^2)^2/\sum\ wF_o^4]^{1/2}$, $w^{-1} = \sigma^2(F_o^2) + 103.36\ F_o^2 + (0.0248\ F_o^2)^2$ for $F_o^2 > 0$ for $Dy_3Cu_2Te_7$ and $w^{-1} = \sigma^2(F_o^2) + (0.04\,F_o^2)^2$ for $F_o^2 > 0$ for $U_2Cu_{0.78}Te_6$, and $w^{-1} = \sigma^2(F_o^2)$ for $F_o^2 \leq 0$ for both compounds.

TABLE 2
Atomic Coordinates and Equivalent Isotropic Displacement Parameters (Å^2) for $Gd_3Cu_2Te_7$ and $U_2Cu_{0.78}Te_6$

Compound	x	y	z	U_{eq}^a
		$Gd_3Cu_2Te_7$		
Gd1	0.26466(5)	0.35657(3)	$\frac{1}{4}$	0.0096(2)
Gd2	0	0.58831(4)	$\frac{1}{4}$	0.0093(2)
Cu1	0	0.7629(1)	$\frac{1}{4}$	0.0307(6)
Cu2^b	0.0696(4)	0.2227(2)	$\frac{1}{4}$	0.055(2)
Te1	0.29924(6)	0.19559(4)	$\frac{1}{4}$	0.0088(2)
Te2	0	0.34793(5)	$\frac{1}{4}$	0.0091(2)
Te3	0	0.11672(4)	0.0001(1)	0.0115(2)
Te4	0.30566(6)	0	0	0.0097(2)
		$U_2Cu_{0.78}Te_6$		
U	0.79226(5)	$\frac{1}{4}$	0.16279(3)	0.0096(1)
Te1	0.26608(9)	$\frac{1}{4}$	0.05932(6)	0.0092(2)
Te2	0.4009(1)	$\frac{1}{4}$	0.66297(6)	0.0133(2)
Te3	0.9061(1)	$\frac{1}{4}$	0.66911(6)	0.0155(2)
Cu^c	0.1000(5)	$\frac{1}{4}$	0.4659(3)	0.012(1)

[a] U_{eq} is defined as one third of the trace of the orthogonalized U_{ij} tensor.

[b] The occupancy of Cu2 is 0.50.

[c] The occupancy of Cu is 0.392(6).

TABLE 3
Selected Bond Lengths (Å) and Angles (deg) for $Gd_3Cu_2Te_7$ and $U_2Cu_{0.78}Te_6$

	$Gd_3Cu_2Te_7$		
Gd1–Te1	3.1114(9)	Cu1–Te3 × 2	2.770(2)
Gd1–Te1 × 2	3.3044(4)	Cu2–Te1	2.691(4)
Gd1–Te2	3.0480(6)	Cu2–Te2	2.530(4)
Gd1–Te3 × 2	3.1517(6)	Cu2–Te3 × 2	2.667(3)
Gd1–Te4 × 2	3.2495(5)	Te3–Te3	3.061(1)
Gd2–Te1 × 2	3.0918(9)	Te3–Te3	3.064(1)
Gd2–Te2 × 2	3.2975(5)	Te4–Te4 × 2	3.0626(2)
Gd2–Te4 × 4	3.1945(6)	Te3–Te3–Te3	180
Cu1–Te1 × 2	2.645(1)	Te4–Te4–Te4	180
	$U_2Cu_{0.78}Te_6$		
U–Te1 × 2	3.1004(6)	Cu–Te3 × 2	2.527(2)
U–Te1	3.2214(8)	Cu–Te3	2.572(3)
U–Te1	3.2358(8)	Te2–Te3	3.028(1)
U–Te2 × 2	3.1233(6)	Te2–Te3	3.073(1)
U–Te3 × 2	3.1403(6)	Te3–Te2–Te3	177.64(3)
Cu–Te2	2.524(3)	Te2–Te3–Te2	177.64(3)

melt cooled. Similar behavior of Cu^+ has been noted in other copper chalcogenides including $\mathrm{KCu}_{7-x}\mathrm{S}_4$ (37, 38), $\mathrm{Mo_3Cu}_{2-x}\mathrm{S}_4$ (39), $\mathrm{K_{1.5}Dy_2Cu_{2.5}Te_5}$ (40), and $Ln\mathrm{Cu}_x\mathrm{Te}_2$ (24, 25). Additional experimental details are shown in Table 1. Table 2 gives positional parameters and equivalent isotropic displacement parameters and Table 3 presents selected bond distances and bond angles.

RESULT AND DISCUSSION

The unit cell of $\mathrm{Gd_3Cu_2Te_7}$ is viewed along the *c* axis in Fig. 1. The compound $\mathrm{Gd_3Cu_2Te_7}$ is isostructural with $\mathrm{DyCu_2Te_7}$ (26). The structure consists of isolated one-dimensional undistorted linear Te chains and two-dimensional ${}^{2}_{\infty}[\mathrm{Cu_2Te_5}]$ layers. These two different structural motifs are separated from one another by Gd atoms. Each Gd atom resides in distorted bicapped trigonal prism of eight Te atoms. Each Cu atom resides in a distorted tetrahedron of four Te atoms; Cu1 is bonded to two Te1 atoms and two Te3 atoms and Cu2 is bonded to one Te1, one Te2, and two Te3 atoms. Such tetrahedral coordination is found in many copper tellurides (24–26). The isolated one-dimensional tellurium chains are composed of an undistorted linear array of Te4 atoms with a Te4–Te4 distance of 3.0626(2) Å (i.e., *c*/2). Moreover, the Te3 atoms also form one-dimensional undistorted linear chains with Te–Te distances of 3.061(1) and 3.064(1) Å (Table 3). The ${}^{2}_{\infty}[\mathrm{Cu_2Te_5}]$ layers are composed of chains of vertex-sharing tetrahedra running along the *c* direction with these Te3 chains forming the central backbone (Fig. 2). The individual tetrahedra are twisted from one another along this central backbone to avoid further tellurium bonding The chains share their Te1 atoms along the *a* axis to form a ${}^{2}_{\infty}[\mathrm{Cu_2Te_5}]$ layer. The remaining crystallographically independent Te atoms, namely Te1 and Te2, are not involved in Te–Te bonding.

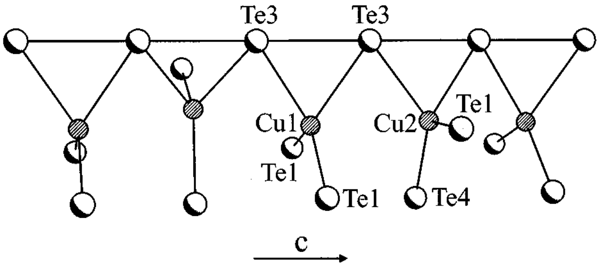

FIG. 2. Vertex-sharing tetrahedral chain of $\mathrm{CuTe_3}$ running along the *c* axis. For clarity, no Gd–Te bonds are drawn in the figure.

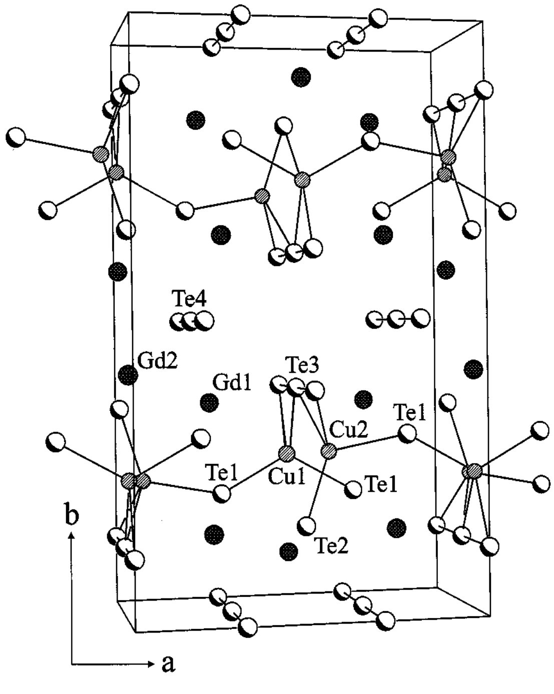

FIG. 1. Unit cell of $\mathrm{Gd_3Cu_2Te_7}$.

The unit cell of $\mathrm{U_2Cu_{0.78}Te_6}$ is viewed along the *b* axis in Fig. 3. This compound is isostructural with $\mathrm{Th_2CuTe_6}$ (31). The structure is also closely related to those of $M\mathrm{Se_3}$ (M = Zr, Th, U) (41–43), $A\mathrm{Th_2}Q_6$ (A = K, Rb, Cs; Q = Se, Te) (28–30), and $\mathrm{Tl_{1.12}U_2Te_6}$ (27). $\mathrm{U_2Cu_{0.78}Te_6}$ comprises the two-dimensional ${}^{2}_{\infty}[\mathrm{UTe_3}]$ slabs stacked along the *c* axis and separated by Cu atoms. In a slab the U atom is coordinated by a bicapped trigonal prism of eight Te atoms. The ${}^{2}_{\infty}[\mathrm{UTe_3}]$ slab is also similar to the ${}^{2}_{\infty}[\mathrm{UTe_3}]$ layer in the structure of α-$\mathrm{UTe_3}$ (19), which belongs to the $\mathrm{ZrSe_3}$ structure type (41). The ternary compounds are obtained by the intercalation of alkali metal or copper atoms into the van der Waals gaps of these binary compounds. The *A* or Tl

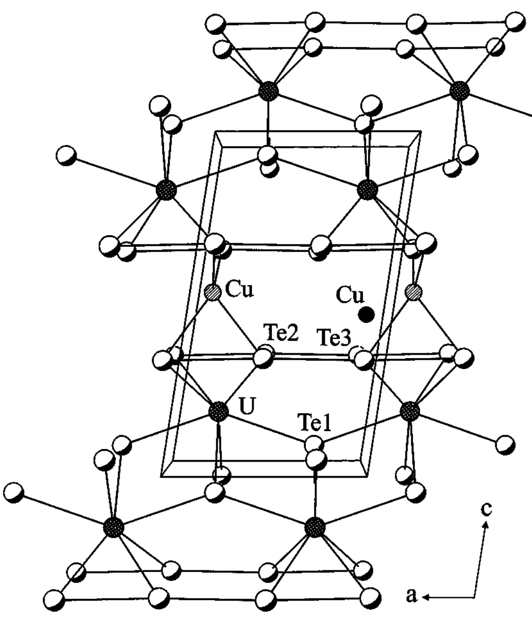

FIG. 3. Unit cell of $\mathrm{U_2Cu_{0.78}Te_6}$. The gray circle represents another disordered Cu position.

TABLE 4
Te–Te Bond Distances and the Oxidation States of Te in Linear Telluride Chains

Compound[a]	Formal oxidation state of Te[b]	Te–Te distances (Å)	Reference
$Cs_5Te_2[Te]$[c]	Te^{-1}	2.808, 3.847	44
$ZrTe[Te_2]$[c]	Te^{-1}	2.793(2), 3.103(2)	45
$UTe[Te]$	$Te^{-(2-\delta)}$	3.057(1), 3.076(1)	19
α-$UTe[Te_2]$	$Te^{-(1-\delta/2)}$	2.751(1), 3.350(1)	19
$U_2Te_2[Te][Te_2]$	$Te^{-(4/3-2/3\delta)}$	3.033(1), 3.047(1); 2.903(1), 3.177(1)	19
$KTh_2Te_2[Te_4]$	$Te^{-1.25}$	3.057(3), 3085(3)	29
$CsTh_2Te_2[Te_4]$	$Te^{-1.25}$	3.052(3), 3.088(3)	28
$Tl_{1.12}U_2Te_2[Te_4]$	$Te^{-(1.28-\delta/2)}$	3.037(2), 3.054(2)	27
$Th_2CuTe_2[Te_4]$[c]	$Te^{-1.25}$	3.058(1), 3.113(1)	31
$U_2Cu_{0.78}Te_2[Te_4]$[c]	$Te^{-(1.2-\delta/2)}$	3.028(1), 3.073(1)	this work
$CsTiUTe_3[Te_2]$	$Te^{-(1.5-\delta/2-\xi/2)}$	3.065(1)	33
$LaCu_{0.40}Te[Te]$	$Te^{-1.40}$	3.1558(5)	25
$DyCu_{0.32}Te[Te]$	$Te^{-1.32}$	3.0273(5)	25
$Dy_3Cu_2Te_3[Te_2][Te_2]$	$Te^{-1.25}$	3.0361(1); 3.0337(6), 3.0386(6)	26
$Gd_3Cu_2Te_3[Te_2][Te_2]$	$Te^{-1.25}$	3.0626(1); 3.061(1), 3.064(1)	this work

[a] The formal oxidation state of Te in the chain is determined from the following oxidation states: Zr, + 4; *Ln*, + 3; Cu, + 1; Te (outside the brackets), − 2; U, + $(4-\delta)$; and Ti, + $(4-\xi)$.

[b] The Te atoms in the linear chains are in the brackets.

[c] The chain is slightly nonlinear.

atom in ATh_2Q_6 or $Tl_{1.12}U_2Te_6$ is coordinated by eight *Q* atoms at the corners of a rectangular parallelepiped. The Cu atom in either $U_2Cu_{0.78}Te_6$ or Th_2CuTe_6 is tetrahedrally coordinated by four Te atoms.

Table 4 lists some compounds in which there are one-dimensional Te chains. The Te ⋯ Te distances fall between those of a Te–Te single bond of 2.76 Å and a $Te^{2-} \cdots Te^{2-}$ van der Waals contact of 4.10 Å. The Te chains of Table 4 can be divided into those that are undistorted (all Te–Te distances the same) and those that are distorted. The formal oxidation states of Te atoms are closely correlated with Te–Te bonding distances. The relationship between the charge on Te and bond distances has been discussed elsewhere (25).

The AnQ_3 and AAn_2Q_6 structures contain $^2_\infty[AnQ_2]$ layers, as shown in Fig. 4a. The distribution of *An* atoms results in two nonequivalent *Q*–*Q* bond distances. This same situation obtains $U_2Cu_{0.78}Te_6$ and Th_2CuTe_6. For $Gd_3Cu_2Te_7$, two kinds of Te chains connected with Gd atoms are displayed in Figs. 4b and 4c. The motif in Fig. 4b can be considered to be a chain in the $^2_\infty[AnQ_2]$ layer, but there is no significant bond alternation in the Te3 chain. Two Te4 chains in Fig. 4c are related to fragments of the $^2_\infty[LnTe]$ layer in $LnTe_2$, and the Te–Te bonds are obviously identical.

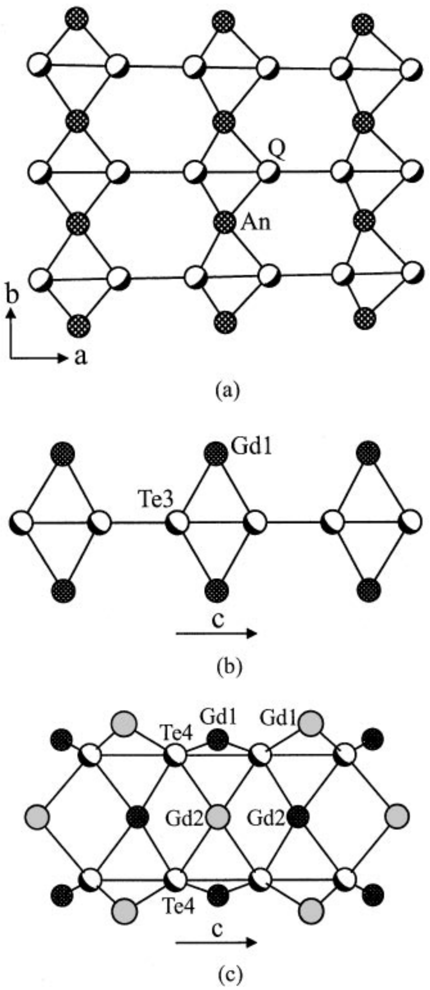

FIG. 4. (a) The $^2_\infty[AnQ_2]$ layer in AAn_2Q_6 and $Cu_xAn_2Te_6$; (b) the fragment relating Te3 chains in $Gd_3Cu_2Te_7$; and (c) the fragment relating two Te4 chains in $Gd_3Cu_2Te_7$.

ACKNOWLEDGMENTS

This research was supported by NSF Grant DMR97-09351. This work made use of facilities supported by the MRSEC program of the National Science Foundation (DMR00-76097) at the Materials Research Center of Northwestern University.

REFERENCES

1. B. Foran, S. Lee, and M. C. Aronson, *Chem. Mater.* **5,** 974–978 (1993).
2. S. Bénazeth, D. Carré, and P. Laruelle, *Acta Crystallogr., Sect. B: Struct. Crystallogr. Cryst. Chem.* **38,** 33–37 (1982).
3. P. Plambeck-Fischer, W. Abriel, and W. Urland, *J. Solid State Chem.* **78,** 164–169 (1989).
4. M. Grupe and W. Urland, *J. Less-Common Met.* **170,** 271–275 (1991).
5. S.-M. Park, S.-J. Park, and S.-J. Kim, *J. Solid State Chem.* **140,** 300–306 (1998).
6. E. DiMasi, B. Foran, M. C. Aronson, and S. Lee, *Chem. Mater.* **6,** 1867–1874 (1994).

7. R. Wang, H. Steinfink, and W. F. Bradley, *Inorg. Chem.* **5,** 142–145 (1966).
8. D. J. Haase, H. Steinfink, and E. J. Weiss, *Inorg. Chem.* **4,** 541–543 (1965).
9. M.-P. Pardo and J. Flahaut, *Bull. Soc. Chim. Fr.* **10,** 3658–3664 (1967).
10. M.-P. Pardo, O. Gorochov, J. Flahaut, and L. Domange, *C. R. Acad. Sci. Paris* **260,** 1666–1669 (1965).
11. D. J. Haase, H. Steinfink, and E. J. Weiss, *Inorg. Chem.* **4,** 538–540 (1965).
12. T. H. Ramsey, H. Steinfink, and E. J. Weiss, *Inorg. Chem.* **4,** 1154–1157 (1965).
13. E. Bucher, K. Andres, F. J. di Salvo, J. P. Maita, A. C. Gossard, A. S. Cooper, and G. W. Hull, *Phys. Rev. B* **11,** 500–513 (1975).
14. W. Lin, H. Steinfink, and E. J. Weiss, *Inorg. Chem.* **4,** 877–881 (1965).
15. W. Tremel and R. Hoffmann, *J. Am. Chem. Soc.* **109,** 124–140 (1987).
16. S. Lee and B. Foran, *J. Am. Chem. Soc.* **116,** 154–161 (1994).
17. H. Noël and J. C. Levet, *J. Solid State Chem.* **79,** 28–33 (1989).
18. A. J. K. Haneveld and F. Jellinek, *J. Less-Common Met.* **21,** 45–49 (1970).
19. K. Stöwe, *J. Alloys Compd.* **246,** 111–123 (1997).
20. O. Tougait, M. Potel, J. Padiou, and H. Noël, *J. Alloys Compd.* **262–263**, 320–324 (1997).
21. R. Patschke, J. Heising, J. Schindler, C. R. Kannewurf, and M. Kanatzidis, *J. Solid State Chem.* **135,** 111–115 (1998).
22. R. Patschke, J. Heising, and M. Kanatzidis, *Chem. Mater.* **10,** 695–697 (1998).
23. R. Patschke, P. Brazis, C. R. Kannewurf, and M. G. Kanatzidis, *J. Mater. Chem.* **9,** 2293–2296 (1999).
24. N.-H. Dung, M.-P. Pardo, and P. Boy, *Acta Crystallogr., Sect. C: Cryst. Struct. Commun.* **39,** 668–670 (1983).
25. F. Q. Huang, P. Brazis, C. R. Kannewurf, and J. A. Ibers, *J. Am. Chem. Soc.* **122,** 80–86 (2000).
26. F. Q. Huang and S. Lee, unpublished data.
27. O. Tougait, A. Daoudi, M. Potel, and H. Noël, *Mater. Res. Bull.* **32,** 1239–1245 (1997).
28. J. A. Cody and J. A. Ibers, *Inorg. Chem.* **35,** 3836–3838 (1996).
29. E. J. Wu, M. A. Pell, and J. A. Ibers, *J. Alloys Compd.* **255,** 106–109 (1997).
30. K.-S. Choi, R. Patschke, S. J. L. Billinge, M. J. Waner, M. Dantus, and M. G. Kanatzidis, *J. Am. Chem. Soc.* **120,** 10706–10714 (1998).
31. A. A. Narducci and J. A. Ibers, *Inorg. Chem.* **37,** 3798–3801 (1998).
32. R. Patschke, P. Brazis, C. R. Kannewurf, and M. Kanatzidis, *J. Mater. Chem.* **8,** 2587–2589 (1998).
33. J. A. Cody and J. A. Ibers, *Inorg. Chem.* **34,** 3165–3172 (1995).
34. “SMART,” Version 5.054 Data Collection and “SAINT-Plus,” Version 6.02A Data Processing Software for the SMART System, Bruker Analytical X-Ray Instruments, Inc., Madison, WI, 2000.
35. G. M. Sheldrick, “SHELXTL,” DOS/Windows/NT, Version 5.10, Bruker Analytical X-Ray Instruments, Inc., Madison, WI, 1997.
36. G. M. Sheldrick, “SHELXTL,” PC Version 5.0, An integrated system for solving, refining, and displaying crystal structures from diffraction data. Siemens Analytical X-Ray Instruments, Inc., Madison, WI, 1994.
37. H. Li, R. Mackay, S.-J. Hwu, Y.-K. Kuo, M. J. Skove, Y. Yokota, and T. Ohtani, *Chem. Mater.* **10,** 3172–3183 (1998).
38. S.-J. Hwu, H. Li, R. Mackay, Y.-K. Kuo, M. J. Skove, M. Mahapatro, C. K. Bucher, J. P. Halladay, and M. W. Hayes, *Chem. Mater.* **10,** 6–9 (1998).
39. K. Yvon, A. Paoli, R. Flükiger, and R. Chevrel, *Acta Crystallogr., Sect. B: Struct. Crystallogr. Cryst. Chem.* **33,** 3066–3072 (1977).
40. F. Q. Huang, W. Choe, S. Lee, and J. S. Chu, *Chem. Mater.* **10,** 1320–1326 (1998).
41. W. Krönert and K. Plieth, *Z. Anorg. Allg. Chem.* **336,** 207–218 (1965).
42. H. Noël, *J. Inorg. Nucl. Chem.* **42,** 1715–1717 (1980).
43. A. B. Salem, A. Meerschaut, and J. Rouxel, *C. R. Acad. Sci., Sér.* 2 **299,** 617–619 (1984).
44. I. Schewe-Miller and P. Böttcher, *Z. Kristallogr.* **196,** 137–151 (1991).
45. S. Furuseth and H. Fjellvåg, *Acta Chem. Scand.* **45,** 694–697 (1991).